Redox Properties and Electrocatalytic Activity of the Oxo/Aqua System $[Ru(terpy)(bpz)(O)]^{2+}/[Ru(terpy)(bpz)(H_2O)]^{2+}$. X-ray Crystal Structure of $[Ru(terpy)(bpz)Cl]PF_6$·MeCN (terpy = 2,2′,2″-Terpyridine; bpz = 2,2′-Bipyrazine)

Alessandra Gerli,[†] Jan Reedijk,*[,†] Miles T. Lakin,[‡] and Anthony L. Spek[‡]

Leiden Institute of Chemistry, Gorlaeus Laboratories, Leiden University, 2300 RA Leiden, The Netherlands, and the Bijvoet Center for Biomolecular Research, Department of Crystal and Structural Chemistry, Utrecht University, 3584 CH Utrecht, The Netherlands

Received September 7, 1994[⊗]

Complexes of the type $[Ru(terpy)(bpz)X]^{n+}$, where terpy = 2,2′,2″-terpyridine, bpz = 2,2′-bipyrazine, and X = Cl^- (**1**), H_2O (**2**), have been prepared and characterized by UV−visible and ^1H NMR spectroscopies, and for the chloride derivative also by X-ray diffraction. $[Ru(terpy)(bpz)Cl]PF_6$·MeCN crystallizes in the triclinic space group $P\bar{1}$ with the following crystallographic parameters: a = 8.9173(4) Å, b = 12.6018(8) Å, c = 13.1743(8) Å, α = 70.392(5)°, β = 81.005(4)°, γ = 76.954(5)°, V = 1353.4(2) Å^3, Z = 2, R_1 = 0.024 [for 5531 reflections $F_o > 4\sigma(F_o)$], and ωR_2 = 0.061 for 6187 unique reflections. The redox properties of **2** have been investigated by electrochemical techniques over the pH range 0−12 in water. Only one reversible voltammetric wave ($E_{1/2}$ = +0.66 V vs SCE at pH = 7) is observed for **2** in the pH range 0−11, which has been assigned to the Ru(II)/Ru(IV) couple. The two-electron nature of the redox process has been confirmed by a spectrophotometric titration of **2** with Ce(IV). The second-order rate constant, k_{cat}, for the oxidation of benzyl alcohol by the electrogenerated $[Ru(IV)(terpy)(bpz)(O)]^{2+}$ was evaluated by cyclic voltammetry. At pH = 11 in phosphate buffer, k_{cat} was estimated to be 23.0(7) M^{-1} s^{-1}. An electrocatalytic rate constant, k_{cat} = 36.1(15) M^{-1} s^{-1}, was measured in 0.1 M NaOH for the oxidation of benzyl alcohol by a related compound, $[Ru(IV)(terpy)(bpy)(O)]^{2+}$, where bpy = 2,2′-bipyridine.

Introduction

High-valent ruthenium oxo complexes are receiving increasing attention in view of their potential as catalysts for the oxidation of polyfunctional molecules such as carbohydrates.[1] As part of a program focused on developing new catalytic systems for the selective oxidation of sugars with acetalic structure,[2,3] we have started investigating the chemistry of oxo ruthenium(IV) complexes[4] based on the 2,2′,2″-terpyridine ligand (terpy).[5]

There has been recently much interest in the synthesis of compounds analogous to $[Ru(terpy)(bpy)(H_2O)]^{2+}$ (bpy = 2,2′-bipyridine),[5] with a focus on the effect that small ligand variations may have on the control, not only of the catalyst reactivity and stability[6,7] but also of the selectivity in the oxidation of polyfunctional substrates.[8] The most widely adopted ligand variations involve replacement of the bpy ligand for another didentate nitrogen-donor ligand having different electronic properties.[6,7] Previous studies have explored the role that electronic properties of ligands have in controlling the redox properties of the ruthenium centers[9,10] and, as a consequence, the reactivity toward oxidation of organic substrates.[11,12]

In the present study, the ligand 2,2′-bipyrazine (bpz) has been chosen to replace bpy in $[Ru(terpy)(bpy)(H_2O)]^{2+}$. Since bpz is a weaker σ-donor than bpy,[13] oxo ruthenium complexes containing bpz are expected to be stronger oxidizing agents than analogous bpy complexes. We report here the synthesis and redox properties of $[Ru(terpy)(bpz)(H_2O)]^{2+}$, which has been found to be an active catalyst for the oxidation of benzyl alcohol when oxidized to its Ru(IV) oxidation state.

Experimental Section

Materials. Bpz was prepared[13] by a literature procedure. $RuCl_3$·$3H_2O$ was obtained as a loan from Johnson Matthey, terpy from Sigma, bpy from Baker, and $(NH_4)_2[Ce(NO_3)_6]$ from Janssen. HPLC-grade CH_3CN used in the voltammetric experiments was purchased by Biosolve Ltd. The water used in the analytical experiments was purified by a Millipore system. All other chemicals were ACS grade and were used without additional purification. Elemental analyses were performed at the University of Groningen, The Netherlands.

Instrumentation and Measurements. ^1H NMR spectra were obtained on a Bruker WM-300 MHz spectrophotometer. For the COSY experiments 256 FID's of eight scans, each consisting of 1K data points, were accumulated. After digital filtering (sine-bell squared) the FID was zero-filled to 512 W in the F_1 dimension. Acquisition parameters were F_1 = ±500 Hz, F_2 = 1000 Hz, and $t_{1/2}$ = 0.001 s; the recycle delay was 1.5 s. Cyclic voltammetric measurements were accomplished with a Bioanalytical System voltammetry controller (EE1011−00) unit. The resulting cyclic voltammograms (CVs) were recorded using a BAS X-Y recorder. A single compartment cell with a three-electrode configuration was used. For aqueous solutions the reference electrode (RE) was a standard calomel electrode (SCE), the auxiliary electrode (AE) was a platinum wire, and the working electrode (WE) was a

[†] Leiden University.
[‡] Utrecht University.
[⊗] Abstract published in *Advance ACS Abstracts*, February 15, 1995.

(1) Koch, H.; Roper, H. *Starch* **1988**, *40*, 121.
(2) Gerli, A.; Reedijk, J. *J. Mol. Catal.* **1994**, *89*, 101.
(3) Boelrijk, A. E. M.; Reedijk, J. *J. Mol. Catal.* **1994**, *89*, 63.
(4) Spek, A; Gerli, A.; Reedijk, J. *Acta Crystallogr.* **1994**, *C50*, 394.
(5) Takeuchi, K. J.; Thompson, M. S.; Pipes, D. W.; Meyer, T. J. *Inorg. Chem.* **1984**, *23*, 1845.
(6) Ho, C.; Che, C.-M.; Lau, T.-C. *J. Chem. Soc., Dalton Trans.* **1990**, 967.
(7) Che, C.-M.; Ho, C.; Lau, T. C. *J. Chem. Soc., Dalton Trans.* **1991**, 1901.
(8) Welch, T. W.; Neyhart, G. A.; Goll, J. G.; Ciftan, S. A.; Thorp, H. H. *J. Am. Chem. Soc.* **1993**, *115*, 9311.
(9) Dovletoglou, A.; Meyer, T. J. *J. Am. Chem. Soc.* **1994**, *116*, 215 and references therein.
(10) Lever, A. B. P. *Inorg. Chem.* **1990**, *29*, 1271.
(11) Raven, S. J.; Meyer, T. J. *Inorg. Chem.* **1988**, *27*, 4478.
(12) Che, C.-M.; Tang, W.-T.; Lee, W.-O.; Wong, K.-Y.; Lau, T.-C. *J. Chem. Soc., Dalton Trans.* **1992**, 1551.
(13) Crutchley, R. J.; Lever, A. B. P. *Inorg. Chem.* **1982**, *21*, 2276.

0020-1669/95/1334-1836$09.00/0

glassy-carbon disk (BAS MF2020) with a surface area of 0.07 cm^2. The WE was polished with alumina before each experiment. For acetonitrile solutions containing 0.1 M tetra-*n*-butylammonium hexafluorophosphate, (TBA)PF_6, as supporting electrolyte, the RE was Ag/AgCl, the AE was a platinum wire, and the WE was a platinum disk (BAS MF2013) with a surface area of 0.02 cm^2. The WE was polished with fine diamond paste (1 μm particle) before each experiment. At the end of each experiment, bis(cyclopentadienyl)iron(II) was added as an internal standard.[14] In order to allow some comparison with the literature data, we point out that under our experimental conditions, $E_{1/2}{}^r$ for the couple bis(cyclopentadienyl)iron(II)/iron(III) was +0.431 V vs Ag/AgCl. Solutions were thoroughly purged with argon and all voltammetric experiments recorded under a positive pressure of this gas at a temperature of 24(1) °C. The $E_{1/2}$ values reported in this work were computed from cyclic voltammetric wave forms as the half-sum of anodic and cathodic peak potentials. Bulk electrolysis experiments employed a Metrohm 641 VA potentiostat and a double-walled Pyrex cell with a glassy-carbon WE. For the electrocatalytic oxidations of benzyl alcohol, the organic products were analyzed on a Hewlett Packard 5700A gas chromatograph equipped with a flame ionization detector and a CP-sil-19CB column (Chrompack). UV−vis spectra were recorded by using either Hewlett Packard 8452A diode array or Varian DMS 200 spectrophotometers with Teflon-stoppered quartz cells having a path length of 1 cm. The acid dissociation constant for [Ru^{II}(terpy)(bpz)(H_2O)]$^{2+}$ to give [Ru^{II}(terpy)(bpz)(OH)]$^+$ was determined spectrophotometrically by using λ = 526 nm. Aliquots of [Ru^{II}(terpy)(bpz)(H_2O)]$^{2+}$ were diluted with a variety of phosphate buffers ranging in the pH 4.8−12 to give final ruthenium concentrations of 1.0×10^{-4} M at 0.1 M ionic strength. Spectrophotometric redox titrations were carried out by adding aliquots of a 2.5×10^{-2} M solution of Ce(IV) in 0.1 M CF_3SO_3H to aliquots (1 mL) of a 1.7×10^{-4} M solution of [Ru^{II}(terpy)(bpz)(H_2O)]$^{2+}$ in 0.1 M CF_3SO_3H. The volume was adjusted to 3 mL by addition of 0.1 M CF_3SO_3H, and the changes in absorbance of the resulting solutions were monitored in the range 200−700 nm. The Ce/Ru mole ratio was varied from 0 to 2.5. Ce(IV) solutions in 0.1 M CF_3SO_3H were prepared with $(NH_4)_2[Ce(NO_3)_6]$ and standardized potentiometrically.[15] The pH of the solutions was determined by using a Schott CG825 pH meter and a Schott combination pH electrode. Buffer solutions for the electrochemical measurements were prepared from aqueous CF_3SO_3H (pH = 0−1), CF_3SO_3H with $NaH_2PO_4 \cdot H_2O$, $Na_2HPO_4 \cdot 7H_2O$, and $Na_3PO_4 \cdot 12H_2O$ (pH = 2−12), and 0.1 M NaOH (pH = 13), to maintain the ionic strength at least at 0.1 M.

Preparations. [Ru(terpy)Cl_3], [Ru(terpy)(bpy)Cl]PF_6, and [Ru(terpy)(bpy)(H_2O)]$(ClO_4)_2$ (**4**) were synthesized following literature procedures.[5,16]

[Ru(terpy)(bpz)Cl]PF_6 (1). [Ru(terpy)Cl_3] (0.4 g, 0.908 mmol) and bpz (0.144 g, 0.908 mmol) were gently refluxed for 9 h in 80 mL of EtOH/H_2O (3/1 v/v) containing LiCl (0.04 g) and triethylamine (0.2 mL) as reductant. The hot solution was filtered and evaporated to dryness. The crude product was dissolved in approximately 40 mL of absolute EtOH and a saturated solution of NH_4PF_6 in absolute EtOH was added. The resulting precipitate was collected, rinsed with absolute EtOH and diethyl ether. The solid was purified by elution from an alumina column with 1/1 CH_2Cl_2/CH_3CN. A burgundy red band, the second to elute after a first orange band, was collected, the solvent removed by rotary evaporation, and the desidered complex recrystallized from CH_3CN added to diethyl ether. Yield: 0.12 g; 20%. Anal. Calcd for $C_{23}H_{17}ClF_6N_7PRu$: C, 41.05; H, 2.55; N, 14.57. Found: C, 41.35; H, 2.87; N, 14.32. UV−vis [λ_{max}/nm(ϵ_{max}/dm^3 mol^{-1} cm^{-1})]: (in acetonitrile) 237 (2.3×10^4), 264 (1.5×10^4), 274 (1.7×10^4), 308 (2.9×10^4), 313 (2.4×10^4), 315 (2.4×10^4), 370 (5.1×10^3) and 513 (9.6×10^3).

[Ru(terpy)(bpz)(H_2O)]$(ClO_4)_2$ (2). **1** (0.084 g, 0.125 mmol) and $AgClO_4$ (0.064 g, 0.309 mmol) were gently refluxed for 3 h in 20 mL of 75% acetone/25% H_2O. After being cooled to room temperature, the mixture was filtered through a fine frit to remove AgCl and $AgPF_6$, and the solution was chilled in the refrigerator overnight. The reaction mixture was again filtered to remove any remaining salt and the volume was slowly reduced to ca. 5 mL by rotary evaporation at 30 °C. The microcrystalline red precipitate was collected, washed with a minimal amount of cold water and air-dried. Yield: 0.080 g, 90%. Anal. Calcd for $C_{23}H_{19}Cl_2N_7O_9Ru$: C, 38.94; H, 2.70; N 13.82. Found: C, 38.56; H, 2.68; N 13.69. UV−vis [λ_{max}/nm(ϵ_{max}/dm^3 mol^{-1} cm^{-1})]: (water) 229 (1.8×10^4), 271 (1.8×10^4), 308 (3.2×10^4), 332 (1.3×10^4), 362 (4.7×10^3) and 494 (7.7×10^3).

Table 1. Crystal Data for [Ru(terpy)(bpz)Cl]PF_6·MeCN

empirical formula: $C_{25}H_{20}ClF_6N_8PRu$	$Z = 2$
fw = 713.98	V = 1353.4(2) Å^3
a = 8.9173(4) Å	t = 150 K
b = 12.6018(8) Å	$R_1{}^a$ = 0.024 [for 5531 reflcns $F_o > 4\sigma(F_o)$]
c = 13.1743(8) Å	$wR_2{}^b$ = 0.061 (for 6187 unique reflcns)
α = 70.392(5)°	weighting scheme^c: $w^{-1} = \sigma(F_o^2) + (0.0350P)^2 + (0.60P)$
β = 81.005(4)°	λ(Mo Kα) = 0.710 73 Å
γ = 76.954(5)°	D_{calcd} = 1.7520(2) g cm^{-3}
space group: $P\bar{1}$ (No. 2)	μ = 8.1 cm^{-1}

^{a} $R_1 = \sum||F_o| - |F_c||/\sum|F_o||$. ^{b} $wR_2 = [\sum[w(F_o^2 - F_c^2)]/\sum[w(F_o^2)^2]]^{1/2}$. ^{c} $P = (MAX(F_o^2, 0) + 2F_c^2)/3$.

X-ray Structure determination of [Ru(terpy)(bpz)Cl]PF_6·MeCN. Crystal data and summarized experimental procedures are collected in Table 1. A crystal suitable for X-ray structure determination was covered by an inert oil, glued to the tip of a glass fiber and immediately placed in the cold nitrogen stream (150 K). Data were collected in $\omega-2\theta$ mode using an Enraf-Nonius CAD4-Turbo diffractometer with a rotating anode. Unit-cell dimensions and standard deviations were obtained by least squared-fit (SET4) to 25 reflections (11.64 < θ < 14.01°). Reduced-cell calculations did not indicate higher lattice symmetry.[17] Three standard reflections were monitored periodically and showed negligible variation in intensity during data collection. The 7547 reflections collected were processed to give 6189 unique reflections (R_{int} = 0.014). These were corrected for Lorentz, polarization and absorption effects. An empirical absorption/extinction correction was applied (DIFABS[18]). No systematic reflection conditions indicates space groups $P1$ or $P\bar{1}$; $P\bar{1}$ was selected and deemed satisfactory by successful refinement. The structure was solved by automated Patterson Methods and subsequent difference Fourier syntheses (DIRDIF[19]). Refinement on F^2 was carried out by full-matrix least-squares techniques (SHELXL-93[20]). Two reflection intensities were deemed spurious and omitted from the calculations, all other reflections were considered observed. Anisotropic thermal parameters were used for all non-hydrogen atoms. Hydrogen atoms were included in the refinement cycle at calculated positions, riding on their carrier atoms. A fixed isotropic displacement parameter of the carrier atom was used for the methyl hydrogen atoms and other hydrogen atoms respectively. Geometric calculations and the ORTEP illustration were performed with PLATON.[21] Computing was conducted on a DECstation 5000 cluster. Final positional parameters are given in Table 2. Listings of thermal parameters, bond distances, bond and torsion angles are included as supplementary material.

Results and Discussion

Structural Studies. An ORTEP drawing of the cation of **1** with the atom-labeling scheme is shown in Figure 1. The ruthenium ligand environment is distorted octahedral with the terpy ligand coordinated, as expected, in meridional fashion,

(14) Gritzner, G.; Kuta, J. *Pure Appl. Chem.* **1984**, *56*, 461.
(15) Vogel, A. I. *A Textbook of Quantitative Inorganic Analysis*; Longmans: London, 1961.
(16) Moyer, B. A.; Meyer, T. J. *J. Am. Chem. Soc.* **1978**, *100*, 3601.
(17) Spek, A. L. *J. Appl. Crystallogr.* **1988**, *21*, 578.
(18) Walker, N.; Stuart, D. *Acta Crystallogr.* **1983**, *A39*, 158.
(19) Beurskens, P. T.; Admiraal, G.; Beurskens, G.; Bosman, W. P.; García-Granda, S.; Gould, R. O.; Smits, J. M. M.; Smykalla, C.; The DIRDIF Program System, Technical Report of the Crystallography Laboratory, University of Nijmegen, The Netherlands, 1992.
(20) Sheldrick, G. M.; SHELXL-93: A Program for Crystal Structure Refinement. University of Göttingen, Germany, 1993.
(21) Spek, A. L. *Acta Crystallogr.* **1990**, *A46*, C34.

Table 2. Atom Coordinates ($\times 10^5$) and Equivalent Isotropic Displacement Coefficients (Å $\times$ 10^4) for [Ru(terpy)(bpz)Cl]PF_6·MeCN

atom	*x*	*y*	*z*	U_{equiv},[a] Å
Ru(1)	84897(2)	18309(1)	22698(1)	145(1)
Cl(2)	68273(5)	23116(4)	37368(3)	205(1)
N(11)	81340(2)	34891(12)	12413(12)	177(4)
N(14)	77650(2)	56357(15)	−3683(15)	332(5)
N(21)	97860(2)	16371(12)	9277(12)	161(4)
N(24)	114930(2)	15739(15)	−10383(13)	259(5)
N(31)	66690(2)	12830(13)	19211(12)	175(4)
N(41)	89200(2)	1969(12)	31147(11)	161(4)
N(51)	104670(2)	17454(13)	29660(12)	183(4)
C(12)	87980(2)	36290(2)	2168(14)	195(5)
C(13)	85870(2)	46920(2)	−5710(2)	268(6)
C(15)	71360(3)	54850(2)	6470(2)	306(6)
C(16)	72880(2)	44360(2)	14470(2)	237(5)
C(22)	97430(2)	25885(15)	413(14)	187(5)
C(23)	105790(4)	25320(2)	−9300(2)	249(5)
C(25)	115510(2)	6550(2)	−1540(2)	221(5)
C(26)	107010(2)	6690(2)	8107(15)	194(5)
C(32)	66790(2)	1359(15)	24109(14)	176(5)
C(33)	55720(2)	−3900(2)	22602(15)	212(5)
C(34)	44190(2)	2550(2)	15900(2)	264(6)
C(35)	43930(2)	14130(2)	11030(2)	270(6)
C(36)	55280(2)	19000(2)	12875(15)	218(5)
C(42)	79760(2)	−4865(15)	30752(14)	174(5)
C(43)	83160(2)	−16570(2)	35953(15)	223(5)
C(44)	96230(2)	−21050(2)	41600(2)	249(5)
C(45)	105710(2)	−13910(2)	42004(15)	218(5)
C(46)	102000(2)	−2280(2)	36629(13)	174(5)
C(52)	110800(2)	6620(2)	35729(14)	184(5)
C(53)	124450(2)	4360(2)	40557(15)	234(5)
C(54)	132060(2)	13260(2)	39100(2)	278(6)
C(55)	125840(2)	24190(2)	33050(2)	282(6)
C(56)	112100(2)	25990(2)	28540(2)	237(5)
P(3)	35339(6)	70025(4)	21773(5)	292(2)
F(4)	50160(2)	75495(13)	15768(12)	446(5)
F(5)	46360(2)	58226(13)	27288(12)	490(5)
F(6)	20580(2)	64705(13)	27629(14)	507(5)
F(7)	36090(2)	74270(2)	31761(14)	587(6)
F(8)	34940(2)	65778(14)	11747(12)	490(5)
F(9)	24390(2)	81860(13)	16240(2)	675(6)

[a] Equivalent isotropic *U* defined as one-third of the trace of the orthogonalized U_{ij} tensor.

the bpz ligand in cis fashion, and the chloride atom trans to one of the bpz nitrogen atoms. Selected bond lengths and angles are reported in Table 3.

The geometrical constraints imposed on the terpy ligand by meridional coordination cause a distinct variation from octahedral geometry. The N(31)−Ru(1)−N(51) angle of approximately 159° and shortening of the Ru(1)−N(41) distance to the central pyridyl of approximately 0.1 Å with respect to Ru−N distances to the two outer pyridyl rings are typical features observed in other Ru(II) terpy structures.[4,22−27]

The Ru(1)−N(11) bond length to the pyrazyl ring trans to the central terpyridine nitrogen is slightly longer than the Ru(1)−N(21) bond length to the pyrazyl ring trans to the chloride atom. This elongation has previously been ascribed to steric interactions between the ligands and not to a trans effect associated with the central terpy nitrogen.[24,25] In a related

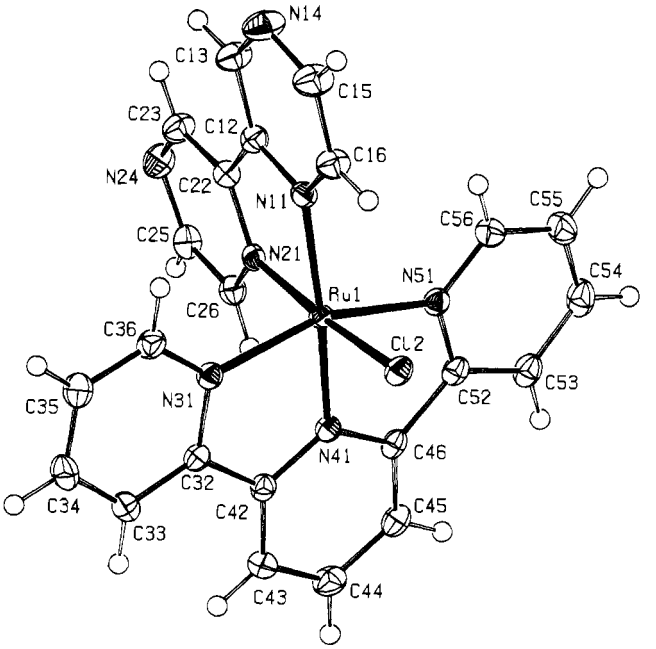

Figure 1. ORTEP drawing (50% probability thermal ellipsoids) and labeling scheme for the non-hydrogen atoms of the cation of **1**.

Table 3. Coordination Lengths (Å) and Angles (deg) for [Ru(terpy)(bpz)Cl]PF_6·MeCN

Bond Lengths			
Ru(1)−Cl(2)	2.4050(5)	Ru(1)−N(31)	2.068(2)
Ru(1)−N(11)	2.059(2)	Ru(1)−N(41)	1.966(2)
Ru(1)−N(21)	2.011(2)	Ru(1)−N(51)	2.077(2)
Bond Angles			
N(11)−Ru(1)−N(21)	78.92(6)	Cl(2)−Ru(1)−N(11)	93.79(5)
N(31)−Ru(1)−N(41)	79.63(7)	Cl(2)−Ru(1)−N(21)	172.66(5)
N(41)−Ru(1)−N(51)	79.01(7)	Cl(2)−Ru(1)−N(31)	87.87(5)
Cl(2)−Ru(1)−N(41)	92.12(5)		
Cl(2)−Ru(1)−N(51)	92.21(5)		

complex, [Ru(terpy)(biq)Cl]PF_6, where biq = 2,2′-biquinoline, differences between the Ru−N distances of the two biquinoline nitrogens were masked by the experimental imprecision.[4]

The Ru−Cl distance of 2.4050(5) Å observed in this structure is slightly longer than that observed[3] in [Ru(terpy)(biq)Cl]PF_6 (2.378(2) Å), but similar to those found in other Ru(II) structures.[28−30]

There is a short intramolecular contact between H(16) and Cl(2) (2.739(3) Å). Analysis of the crystal packing reveals no stacking interaction between neighboring molecules.

To our knowledge, complex **1** is only the second example of a crystal structure of a bipyrazine metal complex, the first being the structure of $[Ru(bpz)_3](PF_6)_2$.[31] In this latter compound the bpz ligands coordinate to ruthenium in a distorted octahedral geometry with average Ru−N bond lengths of 2.051(1) Å.

^{1}H NMR Spectroscopy. The ^{1}H NMR spectrum of **1** is shown in Figure 2. The primed notation refers to the protons of the pyrazyl ring of the bipyrazyl moiety that is trans to the chloride atom. ^{1}H NMR data for complexes **1**, **2**, and $[Ru(terpy)(bpz)(CH_3CN)]^{2+}$ (**3**), obtained by dissolving **2** in

(22) Adcock, P. A.; Keene, F. R.; Smythe, R. S.; Snow, M. R. *Inorg. Chem.* **1984**, *23*, 2336.
(23) Grover, N.; Gupta, N.; Singh, P.; Thorp, H. H. *Inorg. Chem.* **1992**, *31*, 2014.
(24) Hecker, C. R.; Fanwick, P. E.; McMillin, D. R. *Inorg. Chem.* **1991**, *30*, 659.
(25) Leising, R. A.; Kubow, S. A.; Churchill, M. R.; Buttrey, L. A.; Ziller, J. W.; Takeuchi, K. J. *Inorg. Chem.* **1990**, *29*, 1306.
(26) Thummel, R. P.; Jahng, Y. *Inorg. Chem.* **1986**, *25*, 2527.
(27) Gupta, N; Grover, N; Neyhart, G. A.; Liang, W.; Singh, P.; Thorp, H. H. *Angew. Chem., Int. Ed. Engl.* **1992**, *104*, 1058.
(28) Cathey, C. J.; Constable, E. C.; Hannon, M. J.; Tocher, D. A.; Ward, M. D. *J. Chem. Soc., Chem. Commun.* **1990**, 621.
(29) Clear, J. M.; Kelley, J. M.; O'Connell, C. M.; Vos, J. G.; Cardin, C. J.; Costa, S. R.; Edwards, A. J. *J. Chem. Soc., Chem. Commun.* **1980**, 750.
(30) Forster, R. J.; Boyle, A.; Vos, J. G.; Hage, R.; Dijkhuis, A. H. J.; de Graaf, R. A. G.; Haasnoot, J. G.; Prins, R., Reedijk, J. *J. Chem. Soc., Dalton Trans.* **1990**, 121.
(31) Lai, H.; Jones, D. S.; Schwind, D. C.; Rillema, D. P. *J. Crystallogr. Spectrosc. Res.* **1990**, *20*, 321.

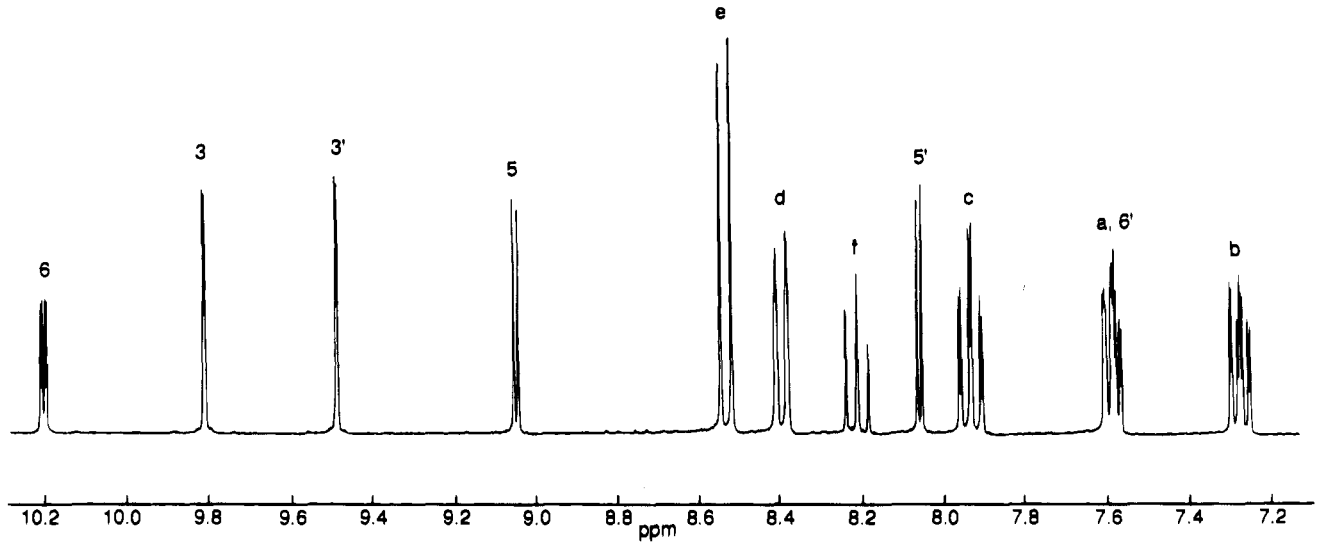

Figure 2. ^{1}H NMR spectrum of **1** (0.02 M) in CD_3CN.

Table 4. ^{1}H NMR Chemical Shifts (ppm) of [Ru(terpy)(bpz)X]$^{n+}$ Complexes

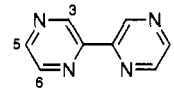

bpz protons

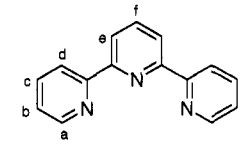

terpy protons

	3	5	6	3′	5′	6′	a	b	c	d	e	f
Cl(**1**)[a]	9.81	9.05	10.20	9.49	8.06	7.58	7.58	7.27	7.93	8.39	8.53	8.21
CH_3CN (**3**)[a]	9.87	9.11	9.67	9.58	8.23	7.46	7.69	7.36	8.05	8.46	8.61	8.40
H_2O (**2**)[b]	9.92	9.13	9.76	9.53	8.07	7.77	7.70	7.38	8.06	8.52	8.68	8.39

[a] In CD_3CN, chemical shifts relative to internal Me_4Si. [b] In D_2O, chemical shifts relative to internal DSS.

acetonitrile, are summarized in Table 4. The spectra of the complexes exhibit 12 resonances, six from the two nonequivalent pyrazyl rings of the bipyrazyl moiety and six from the terpy ligand, as expected for a single plane of symmetry splitting the terpy ligand into equivalent halves.

In the ^{1}H NMR spectrum of **1** (Figure 2), the two doublets of doublets centered at 10.20 and 7.58 ppm which integrate for one proton each can be identified as the two bipyrazyl protons in ortho position (H6, H6′) on the basis of correlation spectroscopy (COSY) and of a nuclear Overhauser enhancement (NOE) from the resonance at 10.20 ppm to that at 9.05 ppm and from the resonance at 7.58 ppm to that at 8.06 ppm. In particular, the signal at 7.58 ppm is assigned to H6′ of the pyrazyl ring of the bipyrazyl ligand trans to the chloride atom. The large upfield shift of this proton with respect to the other bipyrazyl protons is ascribed to the diamagnetic anisotropy of the adjacent terpyridyl rings.[29] The other signal at 10.20 ppm is assigned to H6. This signal shifts upfield (0.53 ppm) upon substitution of the choride atom by an acetonitrile molecule. With the exception of the H6′ signal (0.12 ppm upfield shift) all other signals shift downfield upon substitution of the chloride atom for acetonitrile. The crystal structure of **1** shows that H6 of the bipyrazine moiety has a short intramolecular contact (2.739(3) Å) with the chloride atom. Because of the larger diamagnetic anisotropy of acetonitrile vs chloride, the signal due to H6 is expected to shift upfield in the acetonitrile derivative. Similarly, in the ^{1}H NMR spectrum of $[Ru(bpy)_2(py)Cl]PF_6$ the bipyridyl signal for the H6 closer to the chloride ligand shifts upfield (0.53 ppm) upon susbstitution of the latter for acetonitrile.[32] The assignment of the remaining bipyrazyl protons follows from the COSY spectrum, as well that of the remaining six terpyridyl signals (Table 4). For **1**–**3** both H3 and H5 signals are coupled to the H6 signal ($J_{3,6}$= 1.3 Hz and $J_{5,6}$= 3.3 Hz for **1**), but they are not coupled to each other. The same coupling pattern is observed for the bipyrazyl signals in the ^{1}H NMR spectra[13] of $[Ru(bpz)_3](PF_6)_2$, $[Ru(bpz)_2Cl_2]$ and $[Ru(bpz)_2Cl(CH_3CN)]^{2+}$.

Electronic Absorption Spectra. The absorption spectrum of **2** in aqueous solution is characterized by a visible band at 494 nm which is characteristic for metal-to-ligand charge transfer (MLCT) $d\pi \rightarrow \pi^*$ transitions.[5] The MLCT band shifts to lower energy by 33 nm upon deprotonation of the coordinated water ligand (Figure 3). This red shift in λ_{max} is due to destabilization of the $d\pi$(Ru) electrons by OH^- relative to H_2O, causing the $d\pi \rightarrow \pi^*$ transitions to occur at lower energy.[5] A spectrophotometric titration established that the pK_a value of the coordinated water ligand is 8.8.

A spectrophotometric titration of **2** with Ce(IV) in 0.1 M CF_3SO_3H shows a clean two-electron oxidation of [Ru(II)(terpy)(bpz)$(H_2O)]^{2+}$ to [Ru(IV)(terpy)(bpz)$(O)]^{2+}$ with occurence of an isosbestic point at 366 nm. A plot of the absorbance of **2** at 308 nm (true at other wavelengths as well) vs the Ce/Ru mole ratio is linear with an apparent end point at Ce/Ru mole ratio of 2.

Electrochemical Studies. The CV of $[Ru(terpy)(bpz)Cl]PF_6$ (**1**) in acetonitrile at 0.1 V s^{-1} shows one reversible anodic/cathodic system at +1.09 V vs Ag/AgCl that can be readily assigned to the Ru(II)/Ru(III) couple.[10] The Ru(II)/Ru(III) redox potential of **1** is 370 mV more cathodic than that of the corresponding acetonitrile derivative $[Ru(terpy)(bpz)(CH_3CN)]^{2+}$ (**3**), reflecting the more facile oxidation of the metal

(32) Dobson, J. C.; Helms, J. H.; Doppelt, P.; Sullivan, B. P.; Hatfield, W. E.; Meyer, T. J. *Inorg. Chem.* **1989**, *28*, 2200.

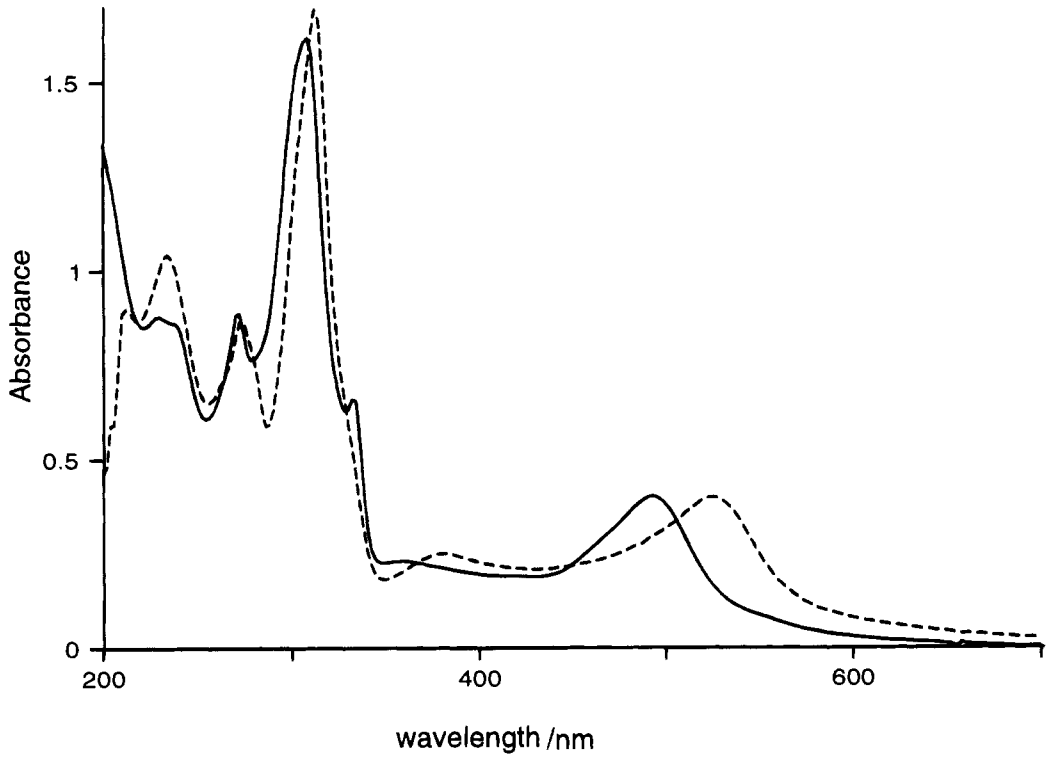

Figure 3. UV−vis spectrum of **2** (5.3×10^{-5} M) in 0.1 M aqueous CF_3SO_3H, pH 1.1(—), and in 0.1 M phosphate buffer, pH 11.5 (- - -).

Table 5. Electrochemical Data for $[Ru(terpy)(N\text{-}N)X]^{n+}$ Derivatives

complex	Ru(II)/Ru(III),[a] V
$[Ru(terpy)(bpz)Cl]PF_6$ (**1**)[b]	1.09
$[Ru(terpy)(bpy)Cl]PF_6$[b]	0.83
$[Ru(terpy)(bpz)CH_3CN)]^{2+}$ (**3**)[b]	1.46
$[Ru(terpy)(bpy)CH_3CN)]^{2+}$ [c]	1.35

[a] Vs Ag/AgCl. All measurements were made in a 0.1 M $(TBA)PF_6$ acetonitrile solution. [b] This work. [c] Reference 10.

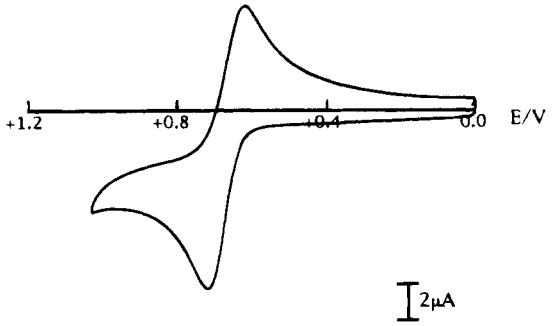

Figure 4. CV of **2** in 0.1 M phosphate buffer, pH 7. Potential (E in V) is vs SCE.

center in the presence of the stronger σ-donor chloride ion. Voltammetric data for compounds **1** and **3**, as well those for analogous bpy complexes, are gathered in Table 5.

A CV of **2** in aqueous solution buffered at pH 7 shows one reversible redox wave (Figure 4). The variation of redox potential for this wave with the pH of the solution is depicted in the Pourbaix diagram[32] of Figure 5. As can be seen from the Pourbaix diagram, two straight lines with different slope can be drawn between the experimental points. The electron−proton content of the redox couples can be determined by comparing the slopes of the experimentally derived lines to values calculated from the Nernst equation expressed in the form $E_{1/2} = E_{1/2}^0 - (0.059m/n)$pH, where m is the number of protons, n is the number of electrons, and $E_{1/2}^0$ is the half-wave potential at pH = 0.[33]

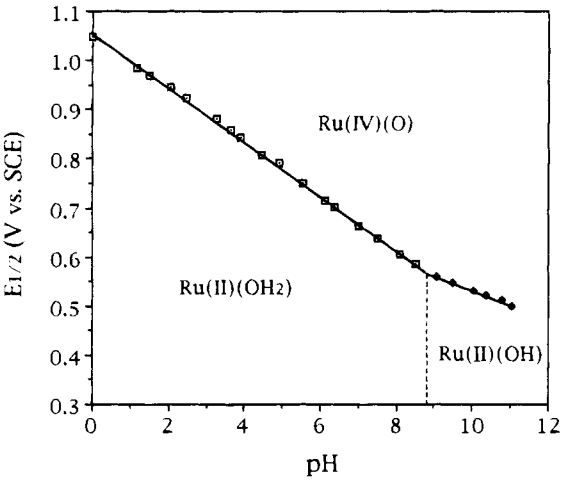

Figure 5. $E_{1/2}$ vs pH (Pourbaix) diagram for **2**. The potential−pH regions of dominant stability for the two oxidation states are indicated as is the pK_a value of **2** by the vertical dashed line.

Between 0 < pH < 8.8 $E_{1/2}$ decreases 60 mV per pH unit, and for pH > 8.8, $E_{1/2}$ decreases 30 mV per pH unit. These data taken together suggest that the observed cyclic voltammetric wave arises from the Ru(II)/Ru(IV) couple. In fact, a 60 mV slope is consistent with a two-proton two-electron oxidative process (eq 1), whereas a 30 mV slope is consistent with the loss of one proton upon two-electron oxidation (eq 2).

$$[Ru^{II}(terpy)(bpz)(H_2O)]^{2+} \rightarrow [Ru^{IV}(terpy)(bpz)(O)]^{2+} + 2H^+ + 2e^- \quad 0 < pH < 8.8 \quad (1)$$

$$[Ru^{II}(terpy)(bpz)(OH)]^{+} \rightarrow [Ru(IV)(terpy)(bpz)(O)]^{2+} + H^+ + 2e^- \quad pH > 8.8 \quad (2)$$

A pK_a value of 8.8 is estimated for **2** from the break point in

(33) Douglas, B.; McDaniel, D. H.; Alexander, J. J. *Concepts and Models of Inorganic Chemistry*; Wiley; New York, 1983.

the $E_{1/2}$ vs pH profile for the Ru(II)/Ru(IV) couple, in excellent agreement with that derived by UV−vis spectrophotometry. At pH = 0, where the Ru(II)/Ru(IV) couple exhibits its most reversible behavior, the separation between cathodic and anodic peaks, ΔE_p, is 50 mV at 0.01 V s^{-1}. From this ΔE_p value and the working tables developed by Taube and Richardson,[34] it is possible to calculate that, if the voltammetric wave is due to two very close one-electron processes (Ru(II)/Ru(III) and Ru(III)/Ru(IV)), they could be separated by as much as 28.6 mV. However, the treatment of Taube and Richardson assumes a strictly Nernstian behavior for the two one-electron waves. The single voltammetric wave observed for **2** is most likely due to a two-electron redox process complicated by slow kinetics at the electrode.[35]

The support for a concerted two-electron process Ru(II)/Ru(IV), as an alternative to two very close one-electron processes, Ru(II)/Ru(III) and Ru(III)/Ru(IV), was provided by the results of a Ce(IV) spectrophotometric experiment. A series of visible spectra were recorded immediately after addition of variable amount of Ce(IV) to different aliquots of **2**, as described in details in the Experimental Section. The linear plot obtained between visible absorbances at selected wavelengths and Ce/Ru mole ratios with an apparent end point at Ce/Ru mole ratio of 2 indicates that the Ru(III) oxidation state is thermodynamically not stable, and therefore, the redox process is a concerted two-electron process. A different type of plot should have been observed if **2** would have been oxidized to the Ru(IV) oxidation state through two distinctive steps. An example of this type is offered by the complex $[Ru(bpy)_2(py)(H_2O)]^{2+}$, which is oxidized to the Ru(IV) oxidation state in two steps, Ru(II)/Ru(III) and Ru(III)/Ru(IV), separated by 210 mV at pH = 0.[36] For this compound the plot of absorbance vs Ce/Ru mole ratio exhibits a break in slope at Ce/Ru mole ratio of 1, corresponding to complete conversion to Ru(III). If the separation between the two consecutive redox steps would be only 28.6 mV, a plot with a less well-defined endpoint should be observed. In fact, under those conditions, equilibrium amounts of Ru(III) and Ru(IV) would be present due to the disproportionation reaction reaction $2Ru(III) \rightleftarrows Ru(IV) + Ru(II)$.

Although the two-electron nature of the redox process was confirmed by both the electrochemical measurements (Pourbaix diagram) and the spectrophotometric experiments with Ce(IV), the number of electrons transferred could not be derived by coulometry. Electrolysis of a solution of **2** in 0.1 M CF_3SO_3H at a platinum electrode held at E_{appl} = +1.2 V vs SCE, lead to extended current/time profiles. Similarly, in a potentiometric titration of **2** using a platinum electrode and Ce(IV) as a redox oxidant a discrete endpoint was not observed. A similar type of behavior has been observed in the potentiometric titration of $[Ru(bpy)_2(py)(H_2O)]^{2+}$ with Ce(IV) and attributed to further uncharacterized reactions with Ce(IV) or surface oxidation of the Pt electrode.[36] Attempts to isolate the complex [Ru(IV)(terpy)(bpz)(O)]$^{2+}$ by addition of an excess or stoichiometric amount of Ce(IV) to an aqueous solution of **2** were unsuccessful. Also after addition of an excess of $NaClO_4$ or NH_4PF_6 to the solution of **2** pretreated with Ce(IV), no precipitate was observed.

The pK_a values of the coordinated water molecule for **2** and a series of related complexes $[Ru(terpy)(N\text{-}N)(H_2O)]^{2+}$ with N-N = bpy,[5] phen,[37] and tmen,[37] where phen = 1,10-phenanthroline and tmen = *N,N,N'*-tetramethylethylenediamine, are compared with their redox potentials in Table 6. The corresponding pK_a values of the free didentate nitrogen donor ligand, p$K_{a(N\text{-}N)}$, are also reported in Table 6. As the σ-donor ability of the didentate nitrogen ligand decreases, or its π-acceptor ability increases, the Ru(II)/Ru(III) and Ru(III)/Ru(IV) redox potentials become more positive, indicating an increase of stabilization of Ru(II) relative to Ru(III) and of Ru(III) relative to Ru(IV). The decrease of redox potentials is also accompanied by a decrease of the pK_a value of the coordinated water molecule. Substitution of the bpy ligand with bpz in $[Ru(terpy)(bpy)(H_2O)]^{2+}$ leads to an increase of redox potential of only 40 mV (Table 6), whereas the same type of substitution in the chloro derivative (Table 5) leads to an increase of the redox potential of 260 mV. Therefore, the presence of aqua ligands results in a relative stabilization of the higher oxidation states. The ability of aqua ligands to stabilize high oxidation states upon deprotonation, is due to an increase of $d\pi(O) \rightarrow d\pi(Ru)$ overlap and formation of multiply bonded oxo groups.[38]

Table 6. $E_{1/2}$ Values at pH 7, pK_a Values of the Coordinated Water Molecule, and p$K_{a(N\text{-}N)}$ Values of the Free N-N Ligand for $[Ru(terpy)(N\text{-}N)(H_2O)]^{2+}$ Complexes

N-N	Ru(II)/Ru(III)[a]	Ru(III)/Ru(IV)[a]	p*K*a	p$K_{a(N\text{-}N)}$
bpz		0.66[b,c]	8.8[c]	0.45[d]
bpy	0.49[e]	0.62[e]	9.7[e]	4.45[d]
phen	0.51[f]	0.61[f]	9.6[f]	4.88[g]
tmen	0.45[f]	0.57[f]	10.2[f]	9.15[g]

[a] Potential is vs SCE for N-N = bpz and vs SSCE for all the other complexes. [b] Ru(II)/Ru(IV). [c] This work. [d] Crutchley, R. J., Kress, N., Lever, A. B. P. *J. Am. Chem. Soc.* **1983**, *105*, 1170. [e] Reference 5. [f] Reference 37. [g] Perrin, D. D. *Dissociation Constants of Organic Bases in Aqueous Solution*; Butterworth: London, 1965.

Interestingly, a good correlation (slope = −1.04, r = 0.996) was found between Ru(III)/Ru(IV) redox potentials for the series of compounds listed in Table 6 (Ru(II)/Ru(IV) for **2**) and the corresponding pK_a values of the free didentate nitrogen donor ligands, p$K_{a(N\text{-}N)}$. A less good correlation was found between Ru(II)/Ru(III) couples and p$K_{a(N\text{-}N)}$ values (slope = −2.38, r = 0.848). It has been recently reported that redox potentials may not be an appropriate measure of the electron density around the metal center for $[Ru(terpy)(N\text{-}N)(H_2O)]^{2+}$ compounds, since these redox potentials are also sterically affected by the didentate nitrogen donor ligands N-N.[39] The excellent correlation found between Ru(III)/Ru(IV) redox potentials and p$K_{a(N\text{-}N)}$ values would suggest that if there is any steric influence of the N-N ligand on the Ru(III)/Ru(IV) redox potential for the compounds listed in Table 6, this has to be approximately the same for bpz, bpy, phen, and tmen. As a consequence, these potentials are primarily sensitive to the electronic properties of the coordinated N-N ligand.

Catalytic Oxidation of Benzyl Alcohol. In order to test the potential applicability of $[Ru^{IV}(terpy)(bpz)(O)]^{2+}$ as an useful electrochemical oxidative catalyst, the electrochemistry of **2** in the presence of benzyl alcohol was studied by cyclic voltammetry. Figure 6 shows a CV of **2** in phosphate buffer, pH = 11, in the presence (dashed curve) and in the absence of benzyl alcohol. The anodic current for the Ru(II)/Ru(IV) wave is replaced by a catalytic current in the presence of benzyl alcohol. No appreciable current is observed in the CV of benzyl alcohol alone under the same conditions. The increase of the anodic current can be explained by the oxidation of benzyl alcohol by

(34) Richardson, D. E.; Taube, H. *Inorg. Chem.* **1981**, *20*, 1278.
(35) Dobson, J. C.; Meyer, T. J. *Inorg. Chem.* **1988**, *27*, 3283.
(36) Moyer, B. A.; Meyer, T. J. *Inorg. Chem.* **1981**, *20*, 436.
(37) Gupta, N.; Grover, N.; Neyahart, G. A.; Singh, P.; Thorp, H. H. *Inorg. Chem.* **1993**, *32*, 310.
(38) Takeuchi, K. J.; Samuels, G. J.; Gersten, S. W.; Gilbert, J. A.; Meyer, T. J. *Inorg. Chem.* **1983**, *22*, 1407.
(39) Bessel, C. A.; Margarucci, J. A.; Acquaye, J. H.; Rubino, R. S. Crandall J.; Jircitano, A. J.; Takeuchi, K. J. *Inorg. Chem.* **1993**, *32*, 5779.

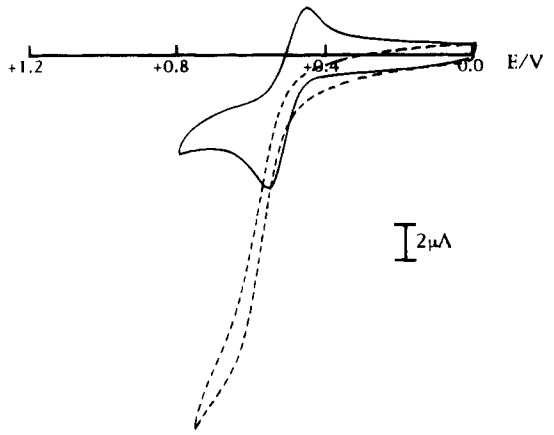

Figure 6. Cyclic voltammogram of **2** (0.5×10^{-3} M) at 0.05 V s^{-1} in 0.1 M phosphate buffer, pH 11, at a glassy carbon electrode, in the absence (—), and in the presence (- - -) of benzyl alcohol (400-fold molar excess). Potential (E in V) is vs SCE.

$[Ru^{IV}(terpy)(bpz)(O)]^{2+}$, which in turn is reduced back to the Ru(II) oxidation form.[40]

Increasing amounts of benzyl alcohol (0.07−0.1−0.15−0.2 M) were added to a solution of **2** (0.5×10^{-3} M) and a series of CVs were recorded at variable scan rates (0.005−0.1 V s^{-1}). As the scan rate decreases the oxidation currents become practically independent of the scan rate. Such behavior is expected in the presence of a large excess of substrate with the electrogenerated catalyst reacting slowly enough to consume very little of the substrate, but rapidly enough to establish a stationary concentration of the catalyst at the electrode surface.[41,42] Under these conditions the net oxidation process is controlled by the catalytic chemical reaction (eq 3),[41,42] where

$$(i_c)_\infty = nFAC_R D^{1/2} k_{cat}^{1/2} C_s^{1/2} \quad (3)$$

n is the number of electron transferred, F is Faraday's constant, D and C_R are the diffusion coefficient and concentration of the catalyst (**2**), respectively, C_s is the substrate concentration (benzyl alcohol), A is the electrode surface area, and k_{cat} is the second-order rate constant.

The determination of k_{cat} by cyclic voltammetry was carried out for solutions at pH approximately two units higher than the pK_a of **2** in order to avoid proton loss from **2** being involved in the pseudo-first-order rate limiting step for benzyl alcohol oxidation (equation 3). k_{cat} could not be determined in more basic solutions, since at higher pH (~ 12) the voltammetric wave of **2** is not well-defined and does not exhibit reversible behavior. The linear plot obtained between experimental limiting currents ($(i_c)_\infty$) and the square root of benzyl alcohol concentration had zero intercept, showing that the catalytic step is pseudo-first-order in benzyl alcohol in agreement with eq 3 (Figure 7). The reaction order with respect to Ru(IV) was presumed to be first order, following the results of previous studies of the oxidation of alcohols by analogous polypyridyl Ru(IV) oxo complexes.[2,43−45] A value of $D = 1.2 \times 10^{-6}$ cm^2 s^{-1} was calculated for the diffusion coefficient of **2** by the Randles−Sevcik equation.[40] A value of $n = 2$ was used in the calculations to account for the two-electron character of the catalyzed reaction.

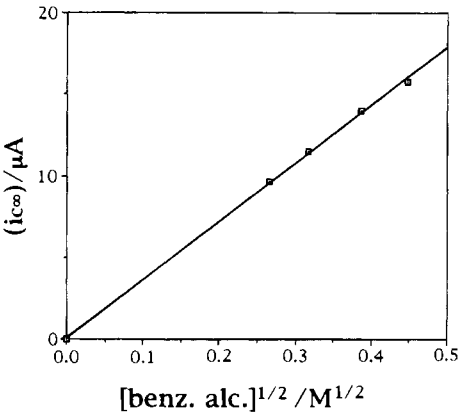

Figure 7. Dependence of the cyclic voltammetric limiting catalytic current $(i_c)_\infty$ for the Ru(II)/Ru(IV) oxidation wave of **2** on the square root of benzyl alcohol concentration.

The rate constant k_{cat} for the oxidation of benzyl alcohol by $[Ru(terpy)(bpz)(O)]^{2+}$ calculated by eq 3 and the voltammetric data is $k_{cat} = 23.0(7)$ M^{-1} s^{-1}.

The experimental determination of k_{cat} for the oxidation of benzyl alcohol was also carried out for $[Ru^{IV}(terpy)(bpy)(O)]^{2+}$ to determine if a variation of the Ru(II)/Ru(IV) redox potential leads to a substantial change in reactivity. Values for $(i_c)_\infty$ were derived from CVs of $[Ru(terpy)(bpy)(H_2O)]^{2+}$ (**4**) (0.5×10^{-3} M) in 0.1 M NaOH at different benzyl alcohol concentrations (0.03, 0.05, 0.07, 0.01, 0.15, 0.2 M). In this case k_{cat} was determined in 0.1 M NaOH (pH 13), since under these conditions $[Ru(terpy)(bpy)(OH)]^{2+}$ is reversibly oxidized in a single two-electron, one-proton step.[5] $D = 3.02 \times 10^{-6}$ cm^2 s^{-1} is the diffusion coefficient of $[Ru(terpy)(bpy)(H_2O)]^{2+}$ (**4**) calculated by the voltammetric data and the Randles−Sevcik equation.[41] Mathematical treatment of the data as described for **2** afforded a value of $k_{cat} = 36.1(15)$ M^{-1} s^{-1} for the oxidation of benzyl alcohol.

Bulk electrolyses of solutions containing 0.2 M benzyl alcohol and 0.5×10^{-3} M catalyst were carried out at a glassy-carbon electrode held at potential 200 mV more positive than the oxidation potential of the catalyst (**2** or **4**). Analysis by GC of the electrolyzed mixtures showed that the oxidation produced benzaldehyde as the only product, just as found previously for related compounds.[43]

The k_{cat} value for the oxidation of benzyl alcohol by $[Ru(terpy)(bpy)(O)]^{2+}$ is not significantly different from that for the oxidation of benzyl alcohol by $[Ru(terpy)(phen)(O)]^{2+}$ ($k_{cat} = 30.8(16)$),[43] a compound having similar redox potential (Table 6). However, **2** which has the highest redox potential, displays also the lowest reactivity. At pH 13 the potential of this compound can be estimated to be 150 and 160 mV higher than that of the bpy and phen derivatives, respectively. The k_{cat} determination was conducted for **2** at a pH two units lower than for the bpy and the phen derivatives. These less basic conditions most likely contributed to lowering the k_{cat} value of **2** in comparison with those for the other two compounds.[44] Nevertheless, the increase in the redox potential of **2** with respect to those for the phen and bpy derivative (approximately 200 mV at the pH at which k_{cat} was measured) is not large enough to compensate for this pH-effect. Therefore, it appears that the redox potential of the Ru(IV) oxidant is not the only factor in determining its reactivity. As suggested by Meyer and coworkers,[44,45] formation of a Ru(IV)=O−alcohol association complex prior to the oxidation could be an important step in determining the overall rate of oxidation. Kinetic studies under identical experimental conditions will be clearly needed to assess

(40) Nicholson, R. S.; Shain, I. *Anal. Chem* **1964**, *36*, 706.
(41) Bard, A. J.; Faulkner, L. R. *Electrochemical Methods*; Wiley; New York, 1980.
(42) Polcyn, D. S.; Shain, I. *Anal. Chem.* **1966**, *38*, 376.
(43) Kutner, W; Meyer, T. J.; Murray, R. W. *J. Electroanal. Chem.* **1985**, *195*, 375.
(44) Roecker, L; Meyer, T. J. *J. Am. Chem. Soc.* **1987**, *109*, 746.
(45) Thompson, M. S.; Meyer, T. J. *J. Am. Chem. Soc.* **1982**, *104*, 4106.

a correlation between driving force and reactivity for this class of compounds.

Concluding Remarks

Replacement of bpy in $[Ru(terpy)(bpy)(H_2O)]^{2+}$ for a weaker σ-donor ligand like bpz leads to a dramatic change of the redox behavior. In particular, the separation of the Ru(II)/Ru(III) and Ru(III)/Ru(IV) couples, observed for the bpy derivative in the pH range 0−11.5, is suppressed in the bpz derivative, and a direct oxidation Ru(II)/Ru(IV) is observed for this latter compound in the same pH range. Comparison of the redox properties of a series compounds of the type $[Ru(terpy)(N\text{-}N)(H_2O)]^{2+}$, where N-N = bpz, bpy, phen, and tmen, shows that both Ru(II)/Ru(III) and Ru(III)/Ru(IV) redox potentials are sensitive to changes in the electronic properties of the N-N ligand, although Ru(II)/Ru(III) potentials appear to be the more significantly affected. The rate constant k_{cat} for the oxidation of benzyl alcohol by $[Ru(terpy)(bpz)(O)]^{2+}$ determined by cyclic voltammetry at pH 11 is of the same order of magnitude as those measured at pH 13 for $[Ru(terpy)(bpy)(O)]^{2+}$ and $[Ru(terpy)(phen)(O)]^{2+}$; however, for the bpz derivative the redox potential is significantly higher than those for the other two derivatives. The relationship between redox properties and reactivity for this class of compounds warrants further study under strictly controlled conditions. The redox studies reported in this paper show that $[Ru(terpy)(bpz)(O)]^{2+}$ is a better two-electron oxidant than $[Ru(terpy)(bpy)(O)]^{2+}$ in the thermodynamic sense. Since one-electron, radical intermediates often have often an indiscriminate chemistry, which can lead to lack of selectivity,[46] it remains to be established whether or not such variation of the redox properties may play a role in influencing the selectivity in reactions like the oxidation of polyfunctional substrates.[8] This issue is currently under investigation.

Acknowledgment. We wish to thank Mr. A. W. M. Lefeber (Leiden University) for recording the COSY NMR spectra, Mr. P. van Os (Utrecht University) for assistance in some electrochemical experiment, Dr. W. P. van Bennekom (Utrecht University) and Dr. Ronald Hage (Unilever Research Laboratory) for comments on the manuscript, and Johnson Matthey Chemical Ltd. (Reading, U.K.) for the generous loan of $RuCl_3$. This work was supported in part (A.G.) by an EC grant (No. ERB4001GT921457, Human Capital and Mobility Programme), and in part (A.L.S.) by the Netherlands Foundation for Chemical Research (SON) with financial aid from the Netherlands Organization for Scientific Research (NWO). M.T.L. thanks the EC for the award of a postdoctoral fellowship under the framework of the Human Capital and Mobility initiative.

Supplementary Material Available: Tables giving details of the X-ray structural data collection, bond lengths and angles, calculated hydrogen atom coordinated and anisotropic thermal parameters, torsion angles for $[Ru(terpy)(bpz)Cl]PF_6 \cdot MeCN$ and figures showing log−log variations of the peak current for the Ru(II)/Ru(IV) oxidation wave of **2** and **4** with potential scan rate at different benzyl alcohol concentations and plot of the dependence of $(i_c)_\infty$ on the square root of benzyl alcohol concentration for **4** (11 pages). Ordering information is given on any current masthead page.

IC941057N

(46) Meyer, T. J. *J. Electrochem. Soc.* **1984**, *7*, 221C.